Molecular Therapy
Nucleic Acids
Original Article

TRIM29 alters bioenergetics of pancreatic cancer cells via cooperation of miR-2355-3p and DDX3X recruitment to AK4 transcript

Liang Hao,[1,2,4] Qi Zhang,[1,2,5] Huai-Yu Qiao,[1] Fu-Ying Zhao,[1] Jing-Yi Jiang,[1] Ling-Yue Huyan,[3] Bao-Qin Liu,[1] Jing Yan,[1] Chao Li,[1] and Hua-Qin Wang[1,2]

[1]Department of Biochemistry and Molecular Biology, China Medical University, Shenyang 110026, China; [2]Key Laboratory of Cell Biology, Ministry of Public Health, and Key Laboratory of Medical Cell Biology, Ministry of Education, China Medical University, Shenyang 110026, China; [3]5+3 integrated clinical medicine 103K, China Medical University, Shenyang 110026, China; [4]Department of Chemistry, China Medical University, Shenyang 110126, China; [5]Criminal Investigation Police University of China, Shenyang 110854, China

TRIM29 is dysregulated in pancreatic cancer and implicated in maintenance of stem-cell-like characters of pancreatic cancer cells. However, the exact mechanisms underlying oncogenic function of TRIM29 in pancreatic cancer cells remain largely unclarified. Using a global screening procedure, the current study found that adenylate kinase 4 (AK4) was profoundly reduced by TRIM29 knockdown. In addition, our data demonstrated that TRIM29 knockdown altered bioenergetics and suppressed proliferation and invasion of pancreatic cancer cells via downregulation of AK4 at the posttranscriptional level. The current study demonstrated that upregulation of microRNA-2355-3p (miR-2355-3p) upregulated AK4 expression via facilitating DDX3X recruitment to the AK4 transcript, and TRIM29 knockdown thereby destabilized the AK4 transcript via miR-2355-3p downregulation. Collectively, our study uncovers posttranscriptional stabilization of the AK4 transcript by miR-2355-3p interaction to facilitate DDX3X recruitment. Regulation of AK4 by TRIM29 via miR-2355-3p thereby provides additional information for further identification of attractive targets for therapy with pancreatic cancer.

INTRODUCTION

Pancreatic adenocarcinoma (PDAC) is a lethal human malignancy characterized by late diagnosis and is unresponsive to chemotherapy and ionizing radiation. PDAC displays the worst prognosis of any major malignancy with a 5-year survival rate of 9%.[1] A better understanding of key signaling mechanisms driving initiation and progression of PDAC may lead to both early diagnosis and intervention.

TRIM29, also known as the ataxia-telangiectasis group D-complementing (ATDC), was first isolated in the screening gene responsible for the genetic disorder ataxia-telangiectasis.[2] TRIM29 belongs to the TRIM protein family and contains the characteristic B1-B2-CC TRIM motifs but lacks the RING finger domain. Accumulating data have demonstrated that TRIM29 is dysregulated in a variety of cancers, and elevated TRIM29 has been associated with dismal prognosis and decreased overall survival of patients with esophageal squamous cell carcinoma.[3,4] TRIM29 is required for the initiation of V-Ki-ras2 Kirsten ratsarcoma viral oncogene homolog (KRAS)-induced pancreatic tumorigenesis[5] and induces an invasive switch in KRAS-induced pancreatic tumorigenesis.[6] Recently we reported that TRIM29 is implicated in maintenance of cancer stem cell (CSC)-like properties of PDAC.[7] In this study, we demonstrated that high TRIM29 immunohistochemical intensity predicted a poor prognosis of patients with PDAC.

The adenylate kinase (AK) family is a class of nucleoside monophosphate kinases that regulates adenine nucleotide metabolism and homeostasis by transferring a phosphate group from one molecule of ATP to AMP to generate 2 molecules of ADP.[8] AK4, a member of the AK family, is distributed in the mitochondrial matrix.[9] AK4 is highly expressed in some cancers and predicts poor clinical outcomes of patients with lung cancer or endometrial cancer.[10–13]

Intrigued by our observation that AK4 was mostly downregulated by TRIM29 knockdown in PDACs, we aimed to clarify in the current study the potential mechanism underlying regulation of AK4 by TRIM29 in pancreatic cancer. Our results uncovered that TRIM29 knockdown suppressed microRNA-2355-3p (miR-2355-3p) expression and subsequently reduced recruitment of DDX3X to the 3′ untranslated region (3′ UTR) of the AK4 transcript. Thereby, the TRIM29/miR-2355-3p/DDX3X/AK4 pathway may provide information for further identification of other targets with therapeutic significance in pancreatic cancer.

RESULTS

TRIM29 and AK4 are positively expressed and predict dismal prognosis of patients with pancreatic cancer

Recently, we have reported that TRIM29 is implicated in maintenance of CSC-like features of PDACs.[7] To further investigate the

Received 16 September 2020; accepted 22 January 2021;
https://doi.org/10.1016/j.omtn.2021.01.027.

Correspondence: Hua-Qin Wang, Department of Biochemistry and Molecular Biology, China Medical University, Shenyang 110026, China.
E-mail: qwang@cmu.edu.cn

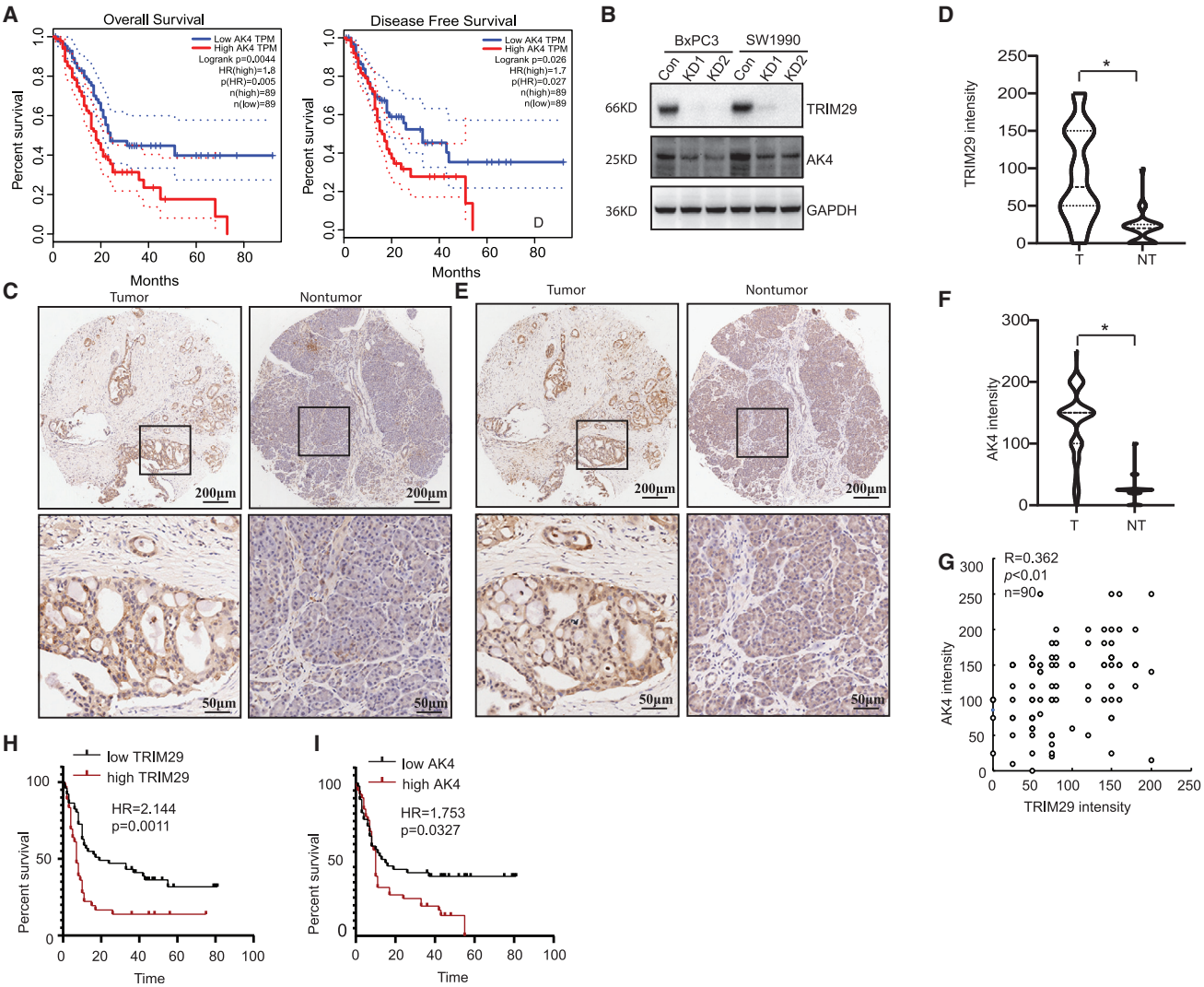

Figure 1. Positive correlation of TRIM29 and AK4 in pancreatic cancers

(A) Correlation between AK4 and overall survival or disease-free survival of patients with pancreatic cancer was analyzed using pancreatic cancer cohort data in The Cancer Genome Atlas (TCGA). (B) TRIM29 was knocked down in BxPC3 and SW1990 cells, and AK4 expression was analyzed using western blot analysis. (C and D) TRIM29 immunohistochemical staining was performed using pancreatic cancer tissue microarray. Representative images were presented (C) and immunohistochemical staining intensities were plotted (D). (E and F) AK4 immunohistochemical staining was performed using pancreatic cancer tissue microarray. Representative images were presented (E) and immunohistochemical staining intensities were plotted (F). (G) Scatterplots showing the positive correlation between TRIM29 and AK4 immunostaining scores in ovarian cancer tissues. Pearson's coefficient tests were used to measure statistical significance. (H and I) Overall survival of patients with pancreatic cancer grouped by TRIM29 (H) or AK4 immunohistochemical intensity was analyzed using Kaplan-Meier plot. *p < 0.05.

mechanisms underlying regulation of CSC-like properties by TRIM29 in PDAC, we performed global proteomics to screen potential molecules involved in the oncogenic function of TRIM29. In BxPC3 cells with TRIM29 knockdown, 37 molecules were downregulated by more than 30% and 8 molecules were upregulated by more than 50% (Table S1). AK4 was most prominently suppressed by TRIM29 knockdown, with a reduction of more than 80% (Table S1). Moreover, pancreatic cancer cohort data in The Cancer Genome Atlas (TCGA) exhibited a poor overall survival and lower disease-free survival of patients with higher AK4 expression (Figure 1A). Western blot confirmed that knockdown of TRIM29 significantly decreased AK4 expression in BxPC3 and SW1990 cells (Figure 1B). Expression of TRIM29 and AK4 was then analyzed using a panel of local pancreatic cancer tissues including 60 pairs of tumor and peripheral nontumor tissues. Immunohistochemistry staining demonstrated that most tumor tissues expressed significantly higher TRIM29 (Figures 1C and 1D) and AK4 (Figures 1E and 1F) compared with their paired nontumor tissues. TRIM29 expression was positively correlated with AK4 expression in a panel of pancreatic cancer tissues (Pearson's coefficient test, r = 0.362, p < 0.01; Figure 1G). Kaplan-Meier survival

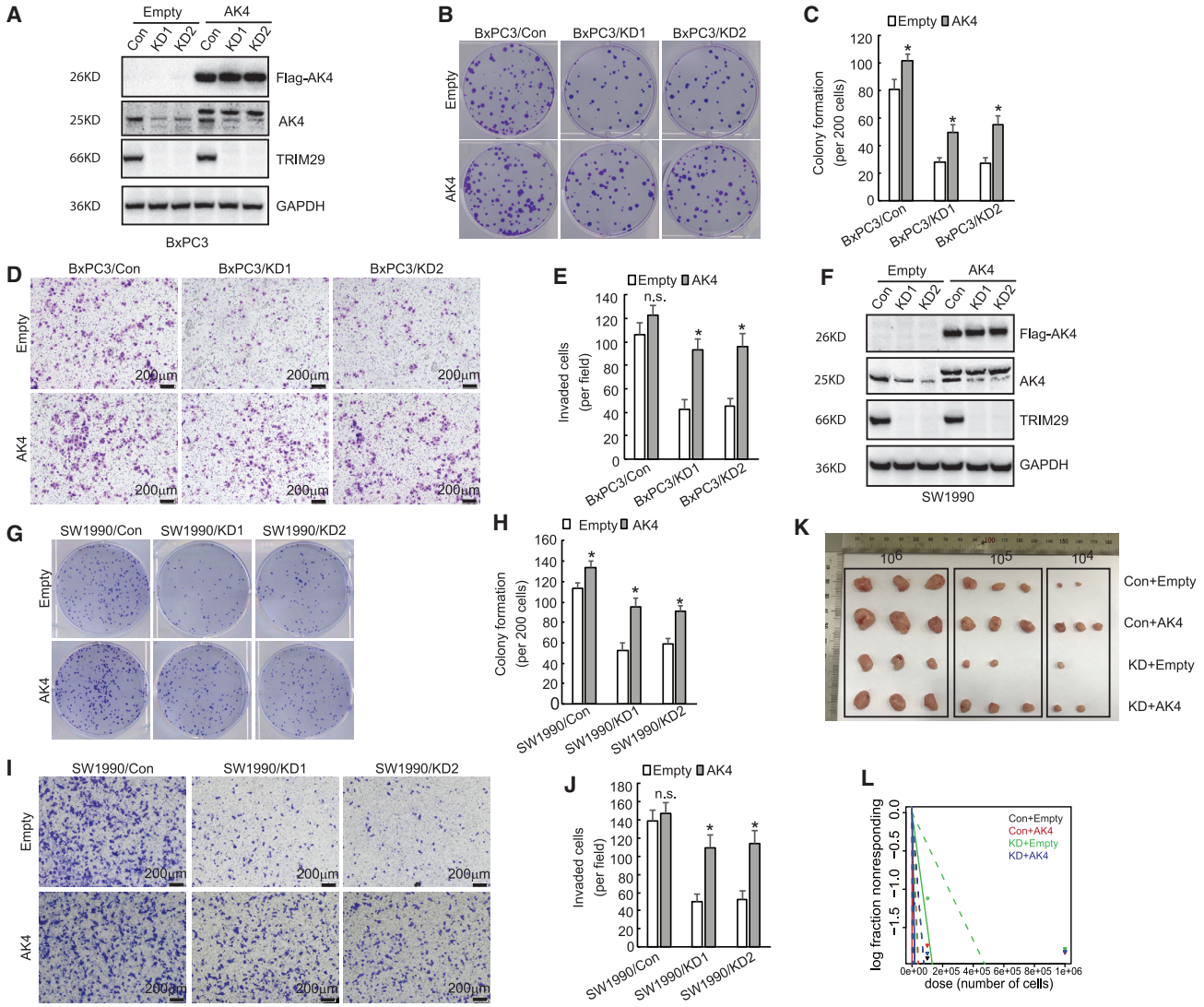

Figure 2. Ectopic AK4 overexpression rescues the suppressive effects of TRIM29 on proliferation and invasion of pancreatic cancer cells

(A–E) Control or TRIM29 knockdown BxPC3 cells were transfected with empty or AK4 construct. (A) Overexpression of AK4 was confirmed by western blot. (B and C) Cell proliferation was analyzed by colony-formation experiments. (D and E) Cell invasion was measured by Transwell analysis. (F–J) Control or TRIM29 knockdown SW1990 cells were transfected with empty or AK4 construct. (F) Overexpression of AK4 was confirmed by western blot. (G and H) Cell proliferation was analyzed by colony-formation experiments. (I and J) Cell invasion was measured by Transwell analysis. (K) The indicated control or TRIM29 knockdown SW1990 cells with serial dilutions containing empty or ectopic expression of AK4 were injected intracutaneously into nude mice. Tumors were excised after the mice were sacrificed on day 28 (n = 3 mice/group). (L) The frequency of CSCs was predicted using ELDA, and a log-fraction plot of the limiting dilution model was extracted. The slope of the line is the log-active cell fraction, and the dotted lines give the 95% confidence interval. *p < 0.05; n.s., not significant.

analysis showed that high TRIM29 (p = 0.0011, hazard ratio [HR] = 2.144; Figure 1H) or AK4 (p = 0.0327, HR = 1.753; Figure 1I) was significantly correlated with poor overall survival of patients with pancreatic cancer.

Ectopic expression of AK4 rescues the suppressive effects of TRIM29 knockdown on proliferation and invasion of PDACs

AK4 was then ectopically introduced into BxPC3 cells (Figure 2A). TRIM29 knockdown decreased colony formation (Figures 2B and 2C) and invasion (Figures 2D and 2E), which was partly blocked by AK4 overexpression (Figures 2B–2E). AK4 was also introduced into SW1990 cells (Figure 2F). Similar to BxPC3 cells, ectopic overexpression of AK4 significantly increased colony formation (Figures 2G and 2H) and invasion (Figures 2I and 2J) of SW1990 cells with TRIM29 knockdown. In addition, TRIM29 knockdown inhibited growth of human pancreatic xenografted tumors in nude mice, which was markedly suppressed by ectopic expression of AK4 (Figure 2K). ELDA, an online tool for limiting dilution analysis (http://bioinf.

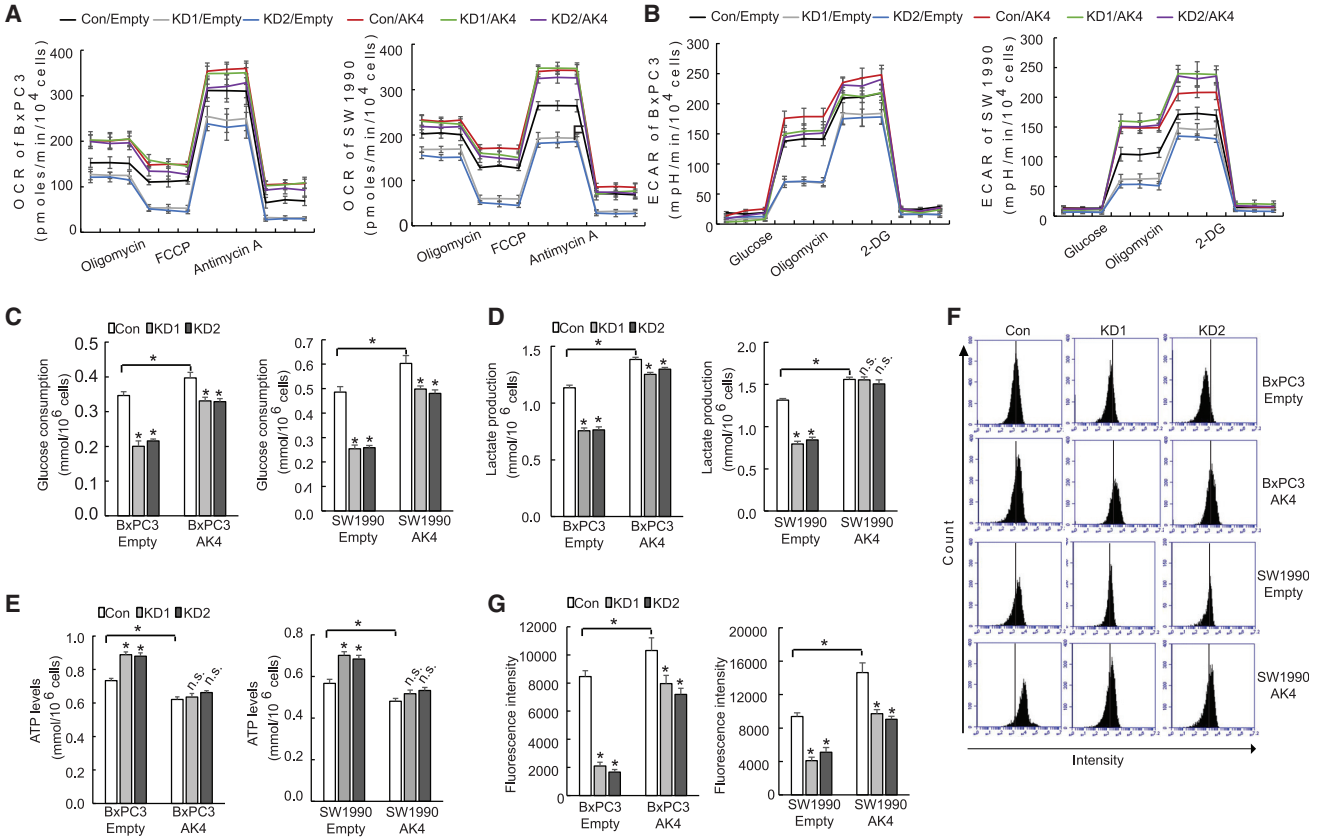

Figure 3. TRIM29 knockdown alters bioenergetics of pancreatic cancer cells via AK4 downregulation

(A) OCR (oxygen consumption rate) was measured using Seahorse instrument according to the manufacturer's instruction. (B) ECAR (extracellular acidification rate) was measured using Seahorse instrument according to the manufacturer's instruction. (C–E) Detailed ECAR was calculated from (B). (F and G) ROS were measured using flow cytometry. *$p < 0.05$.

wehi.edu.au/software/elda/), predicted that a 1/38,953 lower cell frequency was estimated to repopulate control and TRIM29 knockdown cells, while the lower frequency of repopulating TRIM29 knockdown cells was 1/240,210 (Figure 2L). These data indicated that reduction of AK4, at least in part, accounted for reduced proliferation and invasion in PDACs with TRIM29 knockdown.

TRIM29 knockdown increases mitochondrial OXPHOS and decreases glycolysis of PDACs via downregulation of AK4

Biogenetic alterations and mitochondrial dysfunction are major characteristics of cancer. Mitochondrial AK4 is a key regulator in maintaining cellular energy levels.[14] Thereby, the oxygen consumption rates (OCRs) representing the function of mitochondrial OXPHOS and extracellular acidification rates (ECARs) representing the function of glycolysis were simultaneously measured using a seahorse XF24 analyzer. The OCR was significantly decreased by TRIM29 knockdown, while it was increased by ectopic AK4 expression (Figure 3A). TRIM29 knockdown cells exhibited similar OCR levels as control cells when AK4 was ectopically overexpressed (Figure 3A). In detail, TRIM29 knockdown decreased basal OCRs (Figure 1A), proton leak OCRs (Figure S1B), and non-mitochondrial OCRs (Figure S1C), while it increased ATP-linked OCRs (Figure S1D) in both BxPC3 and SW1990 cells. TRIM29 knockdown exhibited no obvious effects on spare OCRs (Figure S1E). Ectopic AK4 expression increased basal OCRs (Figure S1A), while it left unaltered non-mitochondrial OCRs of control BxPC3 and SW1990 cells (Figure S1C). Ectopic AK4 expression demonstrated no constant effects on proton leak OCRs (Figure S1B) or ATP-linked OCRs (Figure S1D) in control BxPC3 and SW1990 cells. In contrast, the effects of TRIM29 knockdown on the detailed OCR partition were completely blocked by ectopic AK4 expression (Figures S1A–S1E). TRIM29 knockdown decreased while AK4 overexpression increased ECARs of BxPC3 and SW1990 cells (Figure 3B). Importantly, TRIM29 knockdown cells exhibited similar ECARs as control cells when AK4 was ectopically expressed (Figure 3B). In addition, TRIM29 knockdown decreased while AK4 overexpression increased glucose consumption (Figure 3C) and lactate release (Figure 3D) of PDACs. The difference between control and TRIM29 knockdown cells was compromised when AK4 was ectopically expressed (Figures 3C and 3D). TRIM29 knockdown increased intracellular ATP levels (Figure 3E), while it decreased reactive oxygen species (ROS; Figures 3F and 3G) in PDACs. On the contrast, AK4

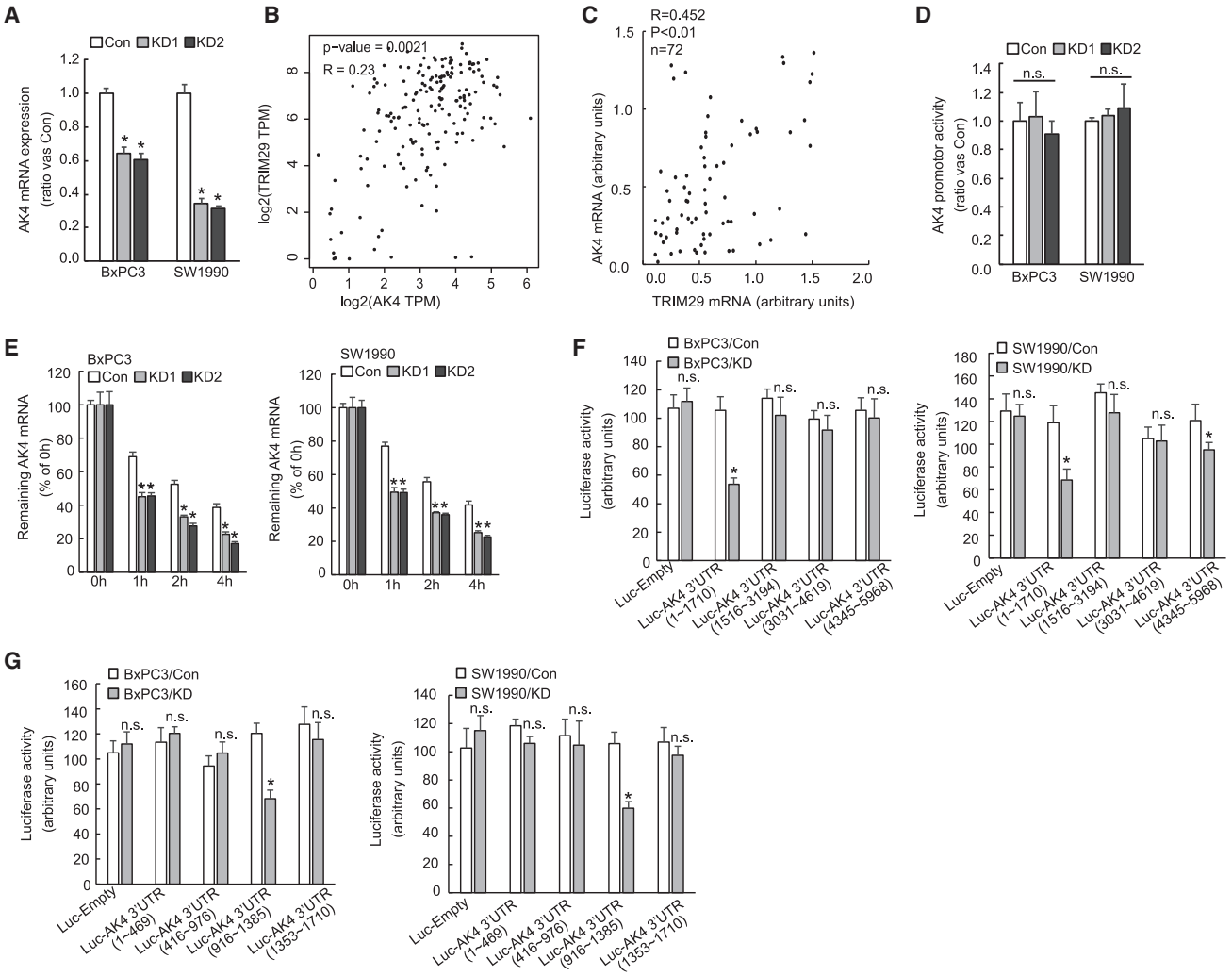

Figure 4. TRIM29 knockdown destabilizes the AK4 transcript via its 3′ UTR

(A) AK4 mRNA expression was analyzed using qRT-PCR in BxPC3 and SW1990 cells with control or TRIM29 knockdown. (B) Correlation between AK4 and TRIM29 transcripts in PDAC tissues was analyzed using pancreatic cancer cohort data in TCGA. (C) Correlation between AK4 and TRIM29 transcripts in PDAC tissues was analyzed using local cohort data. (D) BxPC3 and SW1990 cells with control or TRIM29 knockdown were transfected with luciferase construct containing promoter of AK4, and luciferase activity was analyzed. (E) BxPC3 and SW1990 cells with control or TRIM29 knockdown were incubated with actinomycin D for 0–4 h, and AK4 mRNA expression was analyzed using qRT-PCR. (F and G) Fragments of AK4 3′ UTR were inserted after the stop codon of luciferase reporter gene. BxPC3 and SW1990 cells with control or TRIM29 knockdown were transfected with indicated luciferase reporter construct for 48 h, and luciferase activity was analyzed. *p < 0.05.

overexpression decreased intracellular ATP levels (Figure 3E), while it increased ROS species (Figures 3F and 3G) in PDACs. When AK4 was overexpressed, intracellular ATP levels were unaltered by TRIM29 knockdown (Figure 3E). Collectively, these data indicated that TRIM29 knockdown increased mitochondrial OXPHOS, while it decreased glycolysis of PDACs at least partly via downregulation of AK4.

TRIM29 knockdown destabilizes the AK4 transcript via its 3′ UTR

To explore the potential mechanism underlying regulation of AK4 expression by TRIM29, we performed qRT-PCR and demonstrated that TRIM29 knockdown decreased AK4 mRNA expression in PDACs (Figure 4A). TCGA database (n = 178) showed a positive co-expression of TRIM29 and AK4 transcripts in PDAC tissues (Figure 4B). Data from local cohorts (n = 72) also demonstrated a positive correlation of mRNA expression of TRIM29 and AK4 in pancreatic cancer tissues (Figure 4C). Neither AK4 nascent mRNA synthesis (Figure S2) nor AK4 promoter activity (Figure 4D) was altered by TRIM29 knockdown. Moreover, the stability of AK4 transcripts was measured by exposure to actinomycin D, an RNA biosynthesis inhibitor, for a distinct time and demonstrated that AK4 mRNA stability was significantly decreased by TRIM29 knockdown (Figure 4E). These data indicated that TRIM29 regulated the stability of AK4 mRNA at the posttranscriptional level. UTR,

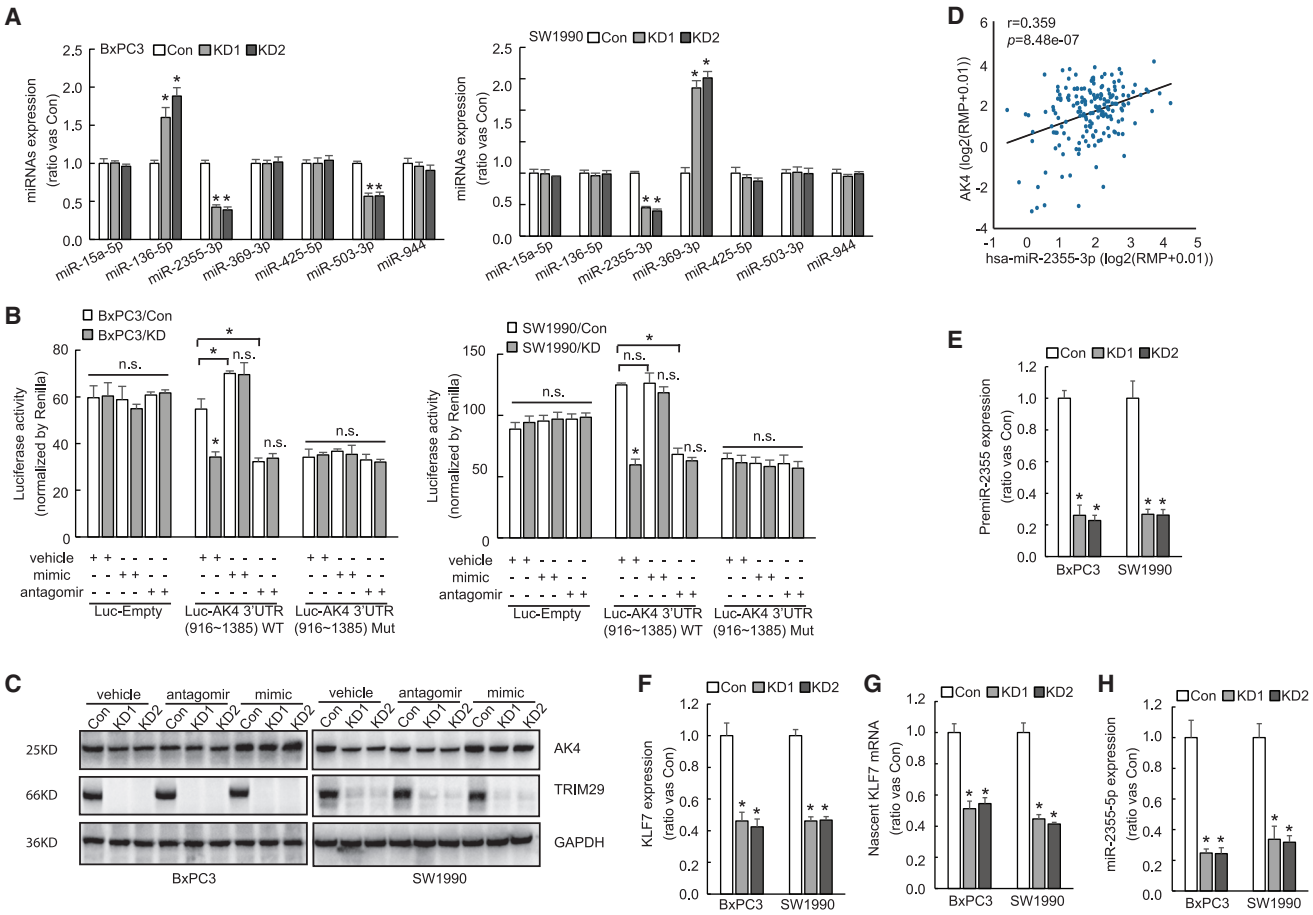

Figure 5. TRIM29 knockdown decreases the stability of the AK4 transcript via reducing miR-2355-3p expression

(A) miR-15a-5p, miR-136-5p, miR-2355-3p, miR-369-3p, miR-425-5p, miR-503-5p, and miR-944 mRNA expressions were analyzed using qRT-PCR in BxPC3 and SW1990 cells with control or TRIM29 knockdown. (B) BxPC3 and SW1990 cells with control or TRIM29 knockdown were cotransfected with miR-2355-3p mimic or antagomir and luciferase containing a wild-type (WT) or potential miR-2355-3p binding site mutant (Mut) 916~1,385 nt fragment of AK4 3′ UTR for 48 h, and luciferase activity was measured. (C) BxPC3 and SW1990 cells with control or TRIM29 knockdown were transfected with control, miR-2355-3p mimic, or antagomir, and AK4 expression was analyzed using western blot analysis. (D) Correlation between AK4 and miR-2355-3p transcript was analyzed using pancreatic cancer cohort data from ENCORI (http://starbase.sysu.edu.cn/). (E) The expression of premiR-2355 was evaluated using qRT-PCR in BxPC3 and SW1990 cells with control or TRIM29 knockdown. (F) The expression of KLF7 was evaluated using qRT-PCR in BxPC3 and SW1990 cells with control or TRIM29 knockdown. (G) The nascent KLF7 mRNA was evaluated using qRT-PCR in BxPC3 and SW1990 cells with control or TRIM29 knockdown. (H) The expression of miR-2355-5p was evaluated using qRT-PCR in BxPC3 and SW1990 cells with control or TRIM29 knockdown. *p < 0.05.

especially 3′ UTR of transcript, contains elements responsible for the stability of target mRNA. The AK4 transcript contains a large 3′ UTR with 5,968 nucleotides (nt), and fragments of AK4 3′ UTR were then inserted just after the stop codon of luciferase reporter gene. Luciferase demonstrated that TRIM29 knockdown consistently decreased the reporter activity of constructs containing the 1~1,710 nt fragment of AK4 3′ UTR in BxPC3 and SW1990 (Figure 4F) cells. Further fragmentation demonstrated that TRIM29 knockdown decreased the reporter activity of constructs containing the 916~1,385 nt fragment of AK4 3′ UTR in BxPC3 and SW1990 cells (Figure 4G). These data indicated that TRIM29 regulated stability of AK4 mRNA via its 3′ UTR, particularly the fragment containing 916~1,385 nt.

TRIM29 knockdown decreases the stability of the AK4 transcript via reducing miR-2355-3p expression

miRNAs regulate the stability of target mRNAs via their 3′ UTR, and bioinformatic analysis using ENCORI (http://starbase.sysu.edu.cn/) predicted a panel of miRNAs interacting with the 916~1,385 nt fragment of AK4 3′ UTR. Among them, miR-15a-5p, miR-136-5p, miR-2355-3p, miR-369-3p, miR-425-5p, miR-503-5p, and miR-944 were screened out because of co-expression with both AK4 and TRIM29 in pancreatic cancer tissues. qRT-PCR demonstrated that only miR-2355-3p was constantly decreased by TRIM29 knockdown in both BxPC3 and SW1990 cells (Figure 5A). Mutant luciferase reporter lack of potential miR-2355-3p binding site was generated. Counterintuitively, miR-2355-3p mimic increased while miR-2355-3p antagomir decreased the

luciferase activity of reporter containing the 916~1,385 nt fragment of AK4 3′ UTR in control BxPC3 and SW1990 cells (Figure 5B). In the presence of miR-2355-3p mimic or antagomir, similar luciferase activity of reporter containing the 916~1,385 nt fragment of AK4 3′ UTR was observed in control and TRIM29 knockdown cells (Figure 5B). Neither miR-2355-3p mimic nor antagomir altered the luciferase activity of reporter containing the 916~1,385 nt fragment of AK4 3′ UTR lack of potential miR-2355-3p binding site (Figure 5B). Western blot confirmed that miR-2355-3p antagomir significantly decreased AK4 expression in control cells, while miR-2355-3p mimic significantly increased AK4 expression in TRIM29 knockdown cells (Figure 5C). Pancreatic cancer cohort data from ENCORI (http://starbase.sysu.edu.cn/) also showed a positive co-expression of miR-2355-3p and the AK4 transcript (Figure 5D). TRIM29 knockdown decreased premiR-2355 (Figure 5E) and its host gene KLF7 (Figure 5F) expression. Nascent RNA isolation demonstrated that TRIM29 knockdown decreased biosynthesis of KLF7 mRNA (Figure 5G). In addition, TRIM29 knockdown also suppressed the expression of miR-2355-5p, the 5′ arm product of pre-miR-2355 (Figure 5H). Collectively, these data indicated that TRIM29 knockdown decreased biogenesis of miR-2355-3p, and miR-2355-3p downregulation was implicated in suppression of AK4 expression by TRIM29 knockdown in pancreatic cancer cells.

TRIM29 knockdown decreases recruitment of DDX3X to the AK4 transcript

Since interaction of miR-2355-3p increased rather than decreased AK4 expression, we turn to ask alternative molecules involved in upregulation of AK4 expression by miR-2355-3p binding DDX3X recruitment. Biotin pull-down using the 916~1,385 nt fragment of AK4 3′ UTR followed by mass spectrometry demonstrated that TRIM29 knockdown altered recruitment of RNA binding proteins (RBPs) DDX3X, ELAVL1, and FKBP4 (Table S2). TCGA dataset demonstrated co-expression of DDX3X, ELAVL1, and FKBP4 with AK4 in PDAC tissues (Figure 6A). RNA immunoprecipitation (RIP) demonstrated that only recruitment of DDX3X was consistently decreased by TRIM29, while recruitment of ELAVL1 or FKBP4 was differently regulated in BxPC3 and SW1990 cells (Figure 6B). TCGA dataset showed that higher DDX3X predicted a poor prognosis of patients with PDAC (Figure 6C). Bioinformatic analysis predicted a potential DDX3X binding sequence spanning 1,233~1,240 nt of AK4 3′ UTR. Mutant reporter construct containing the 916~1,385 fragment of AK4 3′ UTR lacking a potential DDX3X binding site was then generated. Luciferase analysis demonstrated that lack of a DDX3X binding site significantly decreased the luciferase activity in control cells (Figure 6D). Importantly, the luciferase activity of mutant reporter was similar in control and TRIM29 knockdown cells (Figure 6D). Western blot demonstrated that DDX3X expression was unaltered by TRIM29 knockdown (Figure 6E). Knockdown of DDX3X significantly decreased AK4 expression in control BxPC3 and SW1990 cells, while it demonstrated weaker effect in TRIM29 knockdown cells (Figure 6F). These data indicated that TRIM29 knockdown prohibited recruitment of DDX3X to the 3′ UTR of the AK4 transcript, which might be responsible for AK4 downregulation in PDACs.

miR-2355-3p upregulates AK4 expression via facilitating DDX3X recruitment

No interaction was observed between TRIM29 and DDX3X in pancreatic cancer cells (Figure S3A). In addition, TRIM29 was not recruited to the AK4 transcript (Figure S3B). These data excluded the possibility of DDX3X recruitment to the AK4 transcript by TRIM29 directly. Since lack of both a miR-2355-3p binding site (Figure 5B) and a DXX3X binding site (Figure 6D) significantly decreased luciferase activity of reporter containing the 916~1,385 nt fragment of AK4 3′ UTR (Figure 7A), we then asked whether miR-2355-3p upregulated AK4 expression via DDX3X recruitment. Although RIP demonstrated that miR-2355-3p was not enriched in DDX3X-RIPed complex (Figure 7B), miR-2355-3p mimic significantly increased, while miR-2355-3p antagomir significantly decreased DDX3X recruitment to the AK4 transcript (Figure 7C). Combination of miR-2355-3p mimic and DDX3X knockdown was then explored. miR-2355-3p mimic increased AK4 expression when DDX3X was knocked down, and miR-2355-3p was unable to increase AK4 expression of cells with TRIM29 knockdown (Figure 7D). These data indicated that miR-2355-3p upregulated AK4 expression via promotion of DDX3X recruitment to the AK4 transcript. Consistent with AK4 expression, DDX3X knockdown significantly decreased proliferation (Figure 7E) and invasion (Figure 7F) of control cells, which was unaffected by miR-2355-3p mimic (Figures 7E and 7F). On the other hand, miR-2355-3p mimic significantly promoted proliferation (Figure 7E) and invasion (Figure 7F) of pancreatic cells with TRIM29 knockdown, which was blocked by DDX3X knockdown (Figures 7E and 7F).

DISCUSSION

TRIM29 is highly expressed in a variety of tumor types, especially in invasive and aggressive tumors.[15] It has been reported that TRIM29 promotes proliferation and invasion of pancreatic cancer cells through activation of the β-catenin/TCF4 signaling pathway.[16] In addition, TRIM29 functions as a proximal regulator of epithelial mesenchymal transition[6] and plays a critical role in the initiation of KRAS-induced pancreatic tumorigenesis.[5] Recently, we have reported that TRIM29 plays a role in maintenance of CSC-like features of pancreatic cancers.[7] Using a global proteomics method, the current study demonstrated that AK4, a member of adenylate kinase family, was mostly reduced by TRIM29 in PDACs. AK is a key enzyme in transferring a phosphate group from one molecule of ATP or guanosine triphosphate (GTP) to AMP to maintain energy homeostasis in living cells.[8] AK4 is highly expressed in several tumor tissues, which is involved in drug resistance and malignant transformation in cancer.[10,12,17–19] Our data demonstrated that AK4 downregulation was at least partly responsible for the suppressive role of TRIM29 knockdown in proliferation and invasion of PDACs. Through immunohistochemical staining using local pancreatic cancer tissues, we found that TRIM29 and AK4 were highly co-expressed in pancreatic cancer tissues. Consistent with previous report,[20] our data revealed that higher TRIM29 immunohistochemical staining intensity predicted poor prognosis of patients with pancreatic cancers. Both online data from TCGA dataset and our local data demonstrated that a

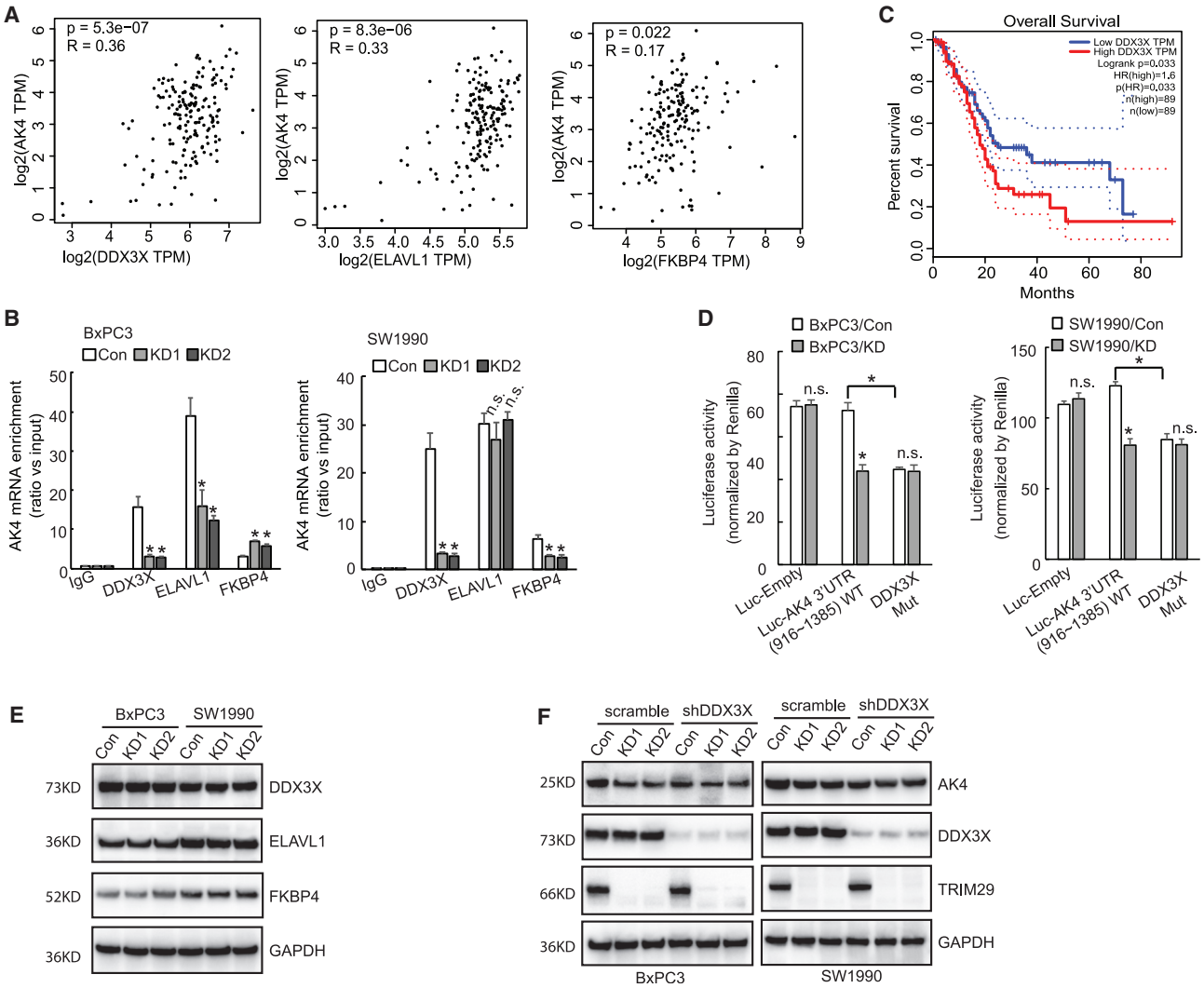

Figure 6. TRIM29 knockdown decreases recruitment of DDX3X to the AK4 transcript

(A) Correlation between DDX3X, ELAVL1, and FKBP4 with the AK4 transcripts in PDAC tissues was analyzed using pancreatic cancer cohort data in TCGA. (B) RIP was performed using immunoglobulin G (IgG), DDX3X, ELAVL1, and FKBP4 antibodies from BxPC3 and SW1990 cells with control or TRIM29 knockdown, and enrichment of AK4 mRNA was evaluated using qRT-PCR. (C) Correlation between DDX3X and overall survival or disease-free survival of patients with pancreatic cancer was analyzed using pancreatic cancer cohort data in TCGA. (D) BxPC3 and SW1990 cells with control or TRIM29 knockdown were transfected with luciferase containing a WT or potential DDX3X binding site Mut 916~1,385 nt fragment of AK4 3′ UTR for 48 h, and luciferase activity was measured. (E) Western blot was performed using the indicated antibodies. (F) DDX3X was knocked down using short hairpin RNAs (shRNAs) specific against DDX3X (shDDX3X), and western blot was performed using the indicated antibodies. *p < 0.05.

high AK4 transcript expression level, as well as its immunohistochemical staining intensity, predicted poor prognosis of patients with pancreatic cancers. Therefore, TRIM29 and AK4 could serve as novel therapeutic targets for the treatment of pancreatic cancer.

3′ UTRs of mRNAs contain regulatory elements, which interact with RBPs and miRNAs, to regulate their own localization, turnover rate, and translation. The AK4 transcript contains a large 3′ UTR fragment, which possesses a variety of potential binding sites for RBPs and miRNAs.[21,22] The current study demonstrated that TRIM29 knockdown reduced recruitment of DDX3X RNA helicase to the 3′ UTR of the AK4 transcript, thereby decreasing the stability of the AK4 transcript. DDX3X is a multifunctional RNA helicase, which belongs to a large family of proteins characterized by containing a DEAD/H (Asp-Glu-Ala-Asp/His) motif and plays a variety functions in RNA metabolism depending on the cellular and signaling context.[23–28] Given the very different functions in RNA metabolism, it is not surprising that DDX3X can potentially play a double-edged function as an oncogene or tumor suppressor in cancer progression.[29–32] Online data from TCGA displayed that higher DDX3X

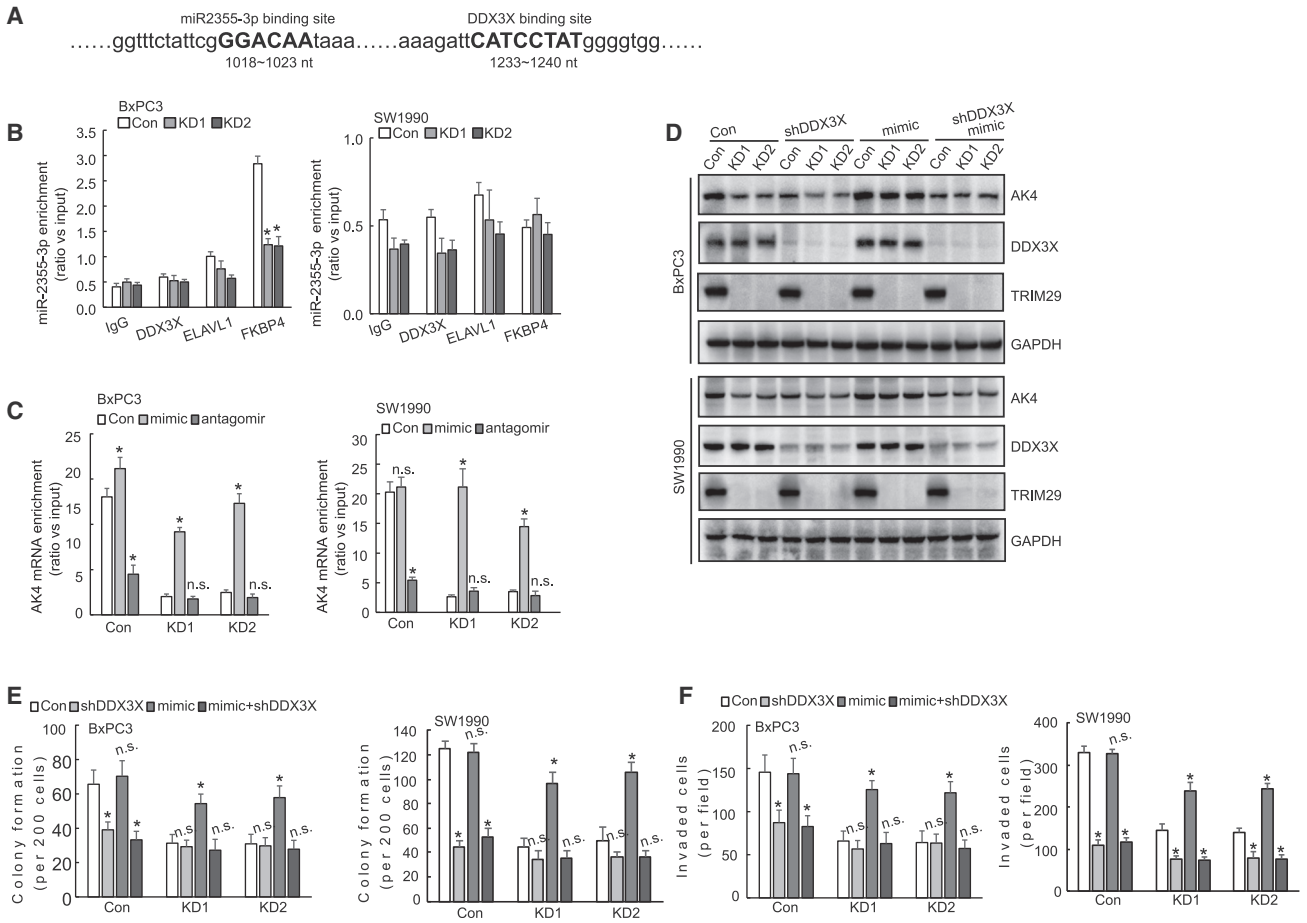

Figure 7. miR-2355-3p upregulates AK4 expression via facilitating DDX3X recruitment

(A) The schematic diagram of AK4 3′ UTR. (B) RIP was performed using IgG, DDX3X, ELAVL1, and FKBP4 antibodies from the indicated cells, and enrichment of miR-2355-3p mRNA was evaluated using qRT-PCR. (C) BxPC3 and SW1990 cells with control or TRIM29 knockdown were transfected with miR-2355-3p mimic or antagomir. RIP was performed using IgG or DDX3X antibody from the indicated cells, and enrichment of AK4 mRNA was evaluated using qRT-PCR. (D–F) Control or TRIM29 knockdown BxPC3 and SW1990 cells infected with control or shDDX3X were transfected with miR-2355-3p mimic. (D) Expression of AK4 was confirmed by western blot. (E) Cell proliferation was analyzed by colony-formation experiments. (F) Cell invasion was measured by Transwell analysis. *$p < 0.05$.

transcript expression is correlated with poor prognosis of patients with pancreatic cancer. In addition, the current study showed that DDX3X was implicated in stabilizing the AK4 transcript via direct interaction. These data suggested an oncogenic role of DDX3X in pancreatic cancer.

The current study demonstrated that TRIM29 knockdown suppressed enrichment of DDX3X in the AK4 transcript without altering its expression, indicating that alternative molecule(s) might be required for recruitment of DDX3X to the AK4 transcript. Our data showed that TRIM29 knockdown decreased miR-2355-3p expression at the transcriptional level, as TRIM29 knockdown decreased its precursor premiR-2355, the 5′ arm product miR-2355-5p of premiR-2355, and its host gene KLF7 expression. The mechanisms underlying regulation of KLF7 at the transcriptional activation by TRIM29 require further investigation. The current study demonstrated that miR-2355-3p antagomirs suppressed while miR-2355-3p mimic promoted interaction of DDX3X with AK4 transcript in control and TRIM29 knockdown cells, respectively. These data indicated that miR-2355-3p was required for the efficient recruitment of DDX3X to the AK4 transcript. miR-2355-3p was not enriched in DDX3X-RIPed complex, indicating that alternative molecules might facilitate miR-2355-3p to recruit DDX3X to the 3′ UTR of the AK4 transcript. In addition, posttranslational modification of DDX3X, for example phosphorylation or ubiquitination, might be responsible for differential recruitment of DDX3X to the 3′ UTR of the AK4 transcript in control and TRIM29 knockdown cells, which requires further investigation in the future. On the contrary to the common image that miRNAs result in degradation or translation suppression of target mRNAs, the current study demonstrated that miR-2355-3p mimic increased AK4 expression in TRIM29 knockdown cells. Consistent with our data, online data from ENCORI displayed positive co-expression of miR-2355-3p with AK4 in

pancreatic cancer tissues. The exact mechanisms by which miR-2355-3p promotes recruitment of DDX3X to the AK4 transcript, as well as their roles in promoting AK4 expression, require further investigation.

Overall, we therefore have a mechanical conclusion of TRIM29 in the progression of PDACs via posttranscriptional regulation of AK4, providing a potential therapeutic target for the treatment of this cancer.

MATERIALS AND METHODS

Cell culture

Human pancreatic cancer cell lines BxPC3 and SW1990 were maintained in DMEM containing 10% fetal bovine serum (FBS) and 100 IU/mL of penicillin and 100 μg/mL of streptomycin. The cells were incubated in a humidified atmosphere at 37°C with 5% CO_2.

Colony-formation assay

For the plate colony-formation assay, 300 cells/well were seeded into 6-well plates (Corning, Acton, MA, USA) and were incubated in a humidified 5% CO_2 incubator at 37°C. After 14 days, cells were fixed with 4% paraformaldehyde for 15 min and stained with 0.1% crystal violet. The colony (containing more than 50 cells) numbers were determined with optical microscopy.

Extracellular flux analysis

A Seahorse XF analyzer (Seahorse Bioscience, Billerica, MA, USA) was employed to analyze the OCRs and ECARs. OCRs and ECARs were reported as absolute rates normalized against counted cell number. The metabolic profile of cells was measured using a Seahorse XF24 analyzer according to the manufacturer's instructions.

Quantitative PCR assay

TRIzol Reagent (Invitrogen, Carlsbad, CA, USA) was used to extract total RNA from cells. Then the RNA was reverse-transcribed by Moloney murine leukemia virus reverse transcriptase (Promega, Madison, WI, USA). Quantitative PCR was performed using the SYBR Ex Taq Kit (Takara, Japan) and the expression levels of AK4 were normalized to the expression of glyceraldehyde-3-phosphate dehydrogenase.

Luciferase reporter assays

Luciferase activity was measured by Dual Luciferase Reporter Gene Assay Kit (Promega, USA). Experiments were performed in triplicates and repeated three times independently. The Renilla luciferase activity values that reflect transfection efficiency were utilized to normalize the firefly luciferase activity values. Data are presented as the mean ± SD (standard deviation) from a representative experiment.

ATP measurement

Cells were grown in a 6-well plate overnight and replaced with fresh complete medium for an additional 24 h. Cell pellets were collected, and ATP amount was quantified using a commercial ATP colorimetric assay kit (BioVision, USA) according to the manufacturer's instruction.

Glucose consumption assay

Cells were grown in a 6-well plate overnight and replaced with fresh complete medium for an additional 24 h. Culture medium was collected, and glucose content was quantified using a glucose colorimetric assay kit (BioVision, USA) according to the manufacturer's instruction.

Lactate release assay

Cells were grown in a 6-well plate overnight and replaced with fresh complete medium for an additional 24 h. Culture medium was collected, and glucose content was quantified using a lactate colorimetric assay kit (BioVision, USA) according to the manufacturer's instruction.

Transwell Matrigel invasion assays

Transwell inserts coated with Matrigel on the upper layers were used for invasion assay. Uncoated inserts were used for migration assay. Briefly, cells were seeded into the upper chamber with FBS-free medium, and the lower chamber was filled with full medium. The cells were incubated in a humidified 5% CO_2 incubator at 37°C. After 24 h, cells in the top chamber were removed, and cells on the underside were fixed in 4% paraformaldehyde for 5 min and then stained with 0.3% crystal violet. Invading cells were counted under a light microscope.

Western blot analysis

Harvested tissues were weighed and homogenized in ice-cold radioimmunoprecipitation assay (RIPA) lysis buffer (50 mM Tris [pH 8.0, 4°C], 200 mM NaCl, 0.5% NP-40, and complete protease inhibitor). To prepare the cells, we washed the cell lines twice with ice-cold PBS, scraped in ice-cold RIPA lysis buffer. Clarified lysate protein concentrations were determined using Bradford reagent (Bio-Rad) before sample normalization for SDS-PAGE electrophoresis using 4%–12% Bis-Tris NuPage gels at 200 V for 60 min. Electrophoresed samples were transferred on nitrocellulose membranes and blocked using 3% BSA dissolved in Tris buffered saline with Tween 20 (TBST; 50 mM Tris [pH 8.0, 4°C], 150 mM NaCl, and 0.1% Tween-20) for 1 h at room temperature. Membranes were then incubated with primary antibodies or biotinylated-vicia villosa lectin (0.2 μg/mL) overnight at 4°C. The next day, membranes were washed three times in TBST before the addition of secondary antibody conjugated with horseradish peroxidase (HRP) or streptavidin-HRP. Membranes were further washed three times with TBST before enhanced chemiluminescence (ECL) exposure.

Tissue microarray and immunohistochemical staining

Tissue microarray sections were purchased from Shanghai Outdo Biotech. Immunohistochemical staining was performed on tissue sections using an antibody against TRIM29 and AK4. A semiquantitative H-score was assessed for each specimen by multiplying the distribution areas (0%–100%) at each staining intensity level by the intensities (0, negative; 1, weak staining; 2, moderate staining; 3, strong staining) as previously reported.[33]

Nude mouse xenograft experiments

BALB/c-nu/nu mice (4 ± 1 week old, 19 ± 5 g weighted, female) were purchased from Liaoning Changsheng Biotechnology. All animal procedures were approved by and compiled with the guidelines of the Institutional Animal Care Committee of China Medical University. The nude mice were housed in plastic polyvinyl chloride (PVC) cage (3 mice in each cage) with sealed air filter, animal isolator, and air laminar flow device, located in an air laminar flow chamber. The ambient temperature was 23°C –24°C, and 12 h of light and dark cycle was maintained daily. Nude mice were randomly divided into three groups. Different groups are for different cell concentrations. The specified number of the indicated cells were resuspended in 100 μL PBS and injected subcutaneously under the left and right back of nude mice, respectively (n = 3 per group). The status of the mice and tumor formation were observed over time, and the mice were sacrificed by cervical dislocation after 28 days. The subcutaneous tumors were removed and photographed.

Statistical analysis

The statistical significance of the difference was analyzed by ANOVA and post hoc Dunnett's test. Statistical significance was defined as $p < 0.05$. For the tissue microarray and immunohistochemical staining, the p value was determined by the log-rank test. All experiments were repeated three times, and data were expressed as the mean ± SD from a representative experiment.

SUPPLEMENTAL INFORMATION

Supplemental information can be found online at https://doi.org/10.1016/j.omtn.2021.01.027.

ACKNOWLEDGMENTS

This work was partly supported by the National Natural Science Foundation of China (32071258, 81902465, and 81872257).

AUTHOR CONTRIBUTIONS

H.-Q.W. designed the study. L.H., Q.Z., B.-Q.L., J.Y., F.-Y.Z., H.-Y.Q., and C.L. performed the experiments and acquired the data. L.H., J.-Y.J., L.-Y.H., B.-Q.L., and H.-Q.W. analyzed and interpreted the acquired data. L.H. and H.-Q.W. participated in scientific discussion and drafting of the paper.

DECLARATION OF INTERESTS

The authors declare no competing interests.

REFERENCES

1. Rahib, L., Smith, B.D., Aizenberg, R., Rosenzweig, A.B., Fleshman, J.M., and Matrisian, L.M. (2014). Projecting cancer incidence and deaths to 2030: the unexpected burden of thyroid, liver, and pancreas cancers in the United States. Cancer Res. *74*, 2913–2921.

2. Kapp, L.N., Painter, R.B., Yu, L.C., van Loon, N., Richard, C.W., 3rd, James, M.R., Cox, D.R., and Murnane, J.P. (1992). Cloning of a candidate gene for ataxia-telangiectasia group D. Am. J. Hum. Genet. *51*, 45–54.

3. Lai, W., Zhao, J., Zhang, C., Cui, D., Lin, J., He, Y., Zheng, H., Wu, X., and Yang, M. (2013). Upregulated ataxia-telangiectasia group D complementing gene correlates with poor prognosis in patients with esophageal squamous cell carcinoma. Dis. Esophagus *26*, 817–822.

4. Harris, T.M., Du, P., Kawachi, N., Belbin, T.J., Wang, Y., Schlecht, N.F., Ow, T.J., Keller, C.E., Childs, G.J., Smith, R.V., et al. (2015). Proteomic analysis of oral cavity squamous cell carcinoma specimens identifies patient outcome-associated proteins. Arch. Pathol. Lab. Med. *139*, 494–507.

5. Wang, L., Yang, H., Zamperone, A., Diolaiti, D., Palmbos, P.L., Abel, E.V., Purohit, V., Dolgalev, I., Rhim, A.D., Ljungman, M., et al. (2019). ATDC is required for the initiation of KRAS-induced pancreatic tumorigenesis. Genes Dev. *33*, 641–655.

6. Wang, L., Yang, H., Abel, E.V., Ney, G.M., Palmbos, P.L., Bednar, F., Zhang, Y., Leflein, J., Waghray, M., Owens, S., et al. (2015). ATDC induces an invasive switch in KRAS-induced pancreatic tumorigenesis. Genes Dev. *29*, 171–183.

7. Sun, J., Yan, J., Qiao, H.-Y., Zhao, F.-Y., Li, C., Jiang, J.-Y., Liu, B.-Q., Meng, X.-N., and Wang, H.-Q. (2020). Loss of TRIM29 suppresses cancer stem cell-like characteristics of PDACs via accelerating ISG15 degradation. Oncogene *39*, 546–559.

8. Panayiotou, C., Solaroli, N., and Karlsson, A. (2014). The many isoforms of human adenylate kinases. Int. J. Biochem. Cell Biol. *49*, 75–83.

9. Miyoshi, K., Akazawa, Y., Horiguchi, T., and Noma, T. (2009). Localization of adenylate kinase 4 in mouse tissues. Acta Histochem. Cytochem. *42*, 55–64.

10. Jan, Y.-H., Tsai, H.-Y., Yang, C.-J., Huang, M.-S., Yang, Y.-F., Lai, T.-C., Lee, C.-H., Jeng, Y.-M., Huang, C.-Y., Su, J.-L., et al. (2012). Adenylate kinase-4 is a marker of poor clinical outcomes that promotes metastasis of lung cancer by downregulating the transcription factor ATF3. Cancer Res. *72*, 5119–5129.

11. Jan, Y.-H., Lai, T.-C., Yang, C.-J., Huang, M.-S., and Hsiao, M. (2019). A co-expressed gene status of adenylate kinase 1/4 reveals prognostic gene signature associated with prognosis and sensitivity to EGFR targeted therapy in lung adenocarcinoma. Sci. Rep. *9*, 12329.

12. Jan, Y.-H., Lai, T.-C., Yang, C.-J., Lin, Y.-F., Huang, M.-S., and Hsiao, M. (2019). Adenylate kinase 4 modulates oxidative stress and stabilizes HIF-1α to drive lung adenocarcinoma metastasis. J. Hematol. Oncol. *12*, 12.

13. Wang, Z.-H., Zhang, Y.-Z., Wang, Y.-S., and Ma, X.-X. (2019). Identification of novel cell glycolysis related gene signature predicting survival in patients with endometrial cancer. Cancer Cell Int. *19*, 296.

14. Lanning, N.J., Looyenga, B.D., Kauffman, A.L., Niemi, N.M., Sudderth, J., DeBerardinis, R.J., and MacKeigan, J.P. (2014). A mitochondrial RNAi screen defines cellular bioenergetic determinants and identifies an adenylate kinase as a key regulator of ATP levels. Cell Rep. *7*, 907–917.

15. Hatakeyama, S. (2016). Early evidence for the role of TRIM29 in multiple cancer models. Expert Opin. Ther. Targets *20*, 767–770.

16. Wang, L., Heidt, D.G., Lee, C.J., Yang, H., Logsdon, C.D., Zhang, L., Fearon, E.R., Ljungman, M., and Simeone, D.M. (2009). Oncogenic function of ATDC in pancreatic cancer through Wnt pathway activation and beta-catenin stabilization. Cancer Cell *15*, 207–219.

17. Zang, C., Zhao, F., Hua, L., and Pu, Y. (2018). The miR-199a-3p regulates the radioresistance of esophageal cancer cells via targeting the AK4 gene. Cancer Cell Int. *18*, 186.

18. Xin, F., Yao, D.-W., Fan, L., Liu, J.-H., and Liu, X.-D. (2019). Adenylate kinase 4 promotes bladder cancer cell proliferation and invasion. Clin. Exp. Med. *19*, 525–534.

19. Zhang, J., Yin, Y.-T., Wu, C.-H., Qiu, R.-L., Jiang, W.-J., Deng, X.-G., and Li, Z.-X. (2019). AK4 Promotes the Progression of HER2-Positive Breast Cancer by Facilitating Cell Proliferation and Invasion. Dis. Markers *2019*, 8186091.

20. Sun, H., Dai, X., and Han, B. (2014). TRIM29 as a novel biomarker in pancreatic adenocarcinoma. Dis. Markers *2014*, 317817.

21. Liu, R., Ström, A.L., Zhai, J., Gal, J., Bao, S., Gong, W., and Zhu, H. (2009). Enzymatically inactive adenylate kinase 4 interacts with mitochondrial ADP/ATP translocase. Int. J. Biochem. Cell Biol. *41*, 1371–1380.

22. Panayiotou, C., Solaroli, N., Johansson, M., and Karlsson, A. (2010). Evidence of an intact N-terminal translocation sequence of human mitochondrial adenylate kinase 4. Int. J. Biochem. Cell Biol. *42*, 62–69.

23. Franca, R., Belfiore, A., Spadari, S., and Maga, G. (2007). Human DEAD-box ATPase DDX3 shows a relaxed nucleoside substrate specificity. Proteins *67*, 1128–1137.

24. Heerma van Voss, M.R., Vesuna, F., Bol, G.M., Afzal, J., Tantravedi, S., Bergman, Y., Kammers, K., Lehar, M., Malek, R., Ballew, M., et al. (2018). Targeting mitochondrial translation by inhibiting DDX3: a novel radiosensitization strategy for cancer treatment. Oncogene *37*, 63–74.

25. Chen, H.-H., Yu, H.-I., Yang, M.-H., and Tarn, W.-Y. (2018). DDX3 Activates CBC-eIF3-Mediated Translation of uORF-Containing Oncogenic mRNAs to Promote Metastasis in HNSCC. Cancer Res. *78*, 4512–4523.

26. Cannizzaro, E., Bannister, A.J., Han, N., Alendar, A., and Kouzarides, T. (2018). DDX3X RNA helicase affects breast cancer cell cycle progression by regulating expression of KLF4. FEBS Lett. *592*, 2308–2322.

27. Sharma, D., and Jankowsky, E. (2014). The Ded1/DDX3 subfamily of DEAD-box RNA helicases. Crit. Rev. Biochem. Mol. Biol. *49*, 343–360.

28. Soto-Rifo, R., and Ohlmann, T. (2013). The role of the DEAD-box RNA helicase DDX3 in mRNA metabolism. Wiley Interdiscip. Rev. RNA *4*, 369–385.

29. He, Y., Zhang, D., Yang, Y., Wang, X., Zhao, X., Zhang, P., Zhu, H., Xu, N., and Liang, S. (2018). A double-edged function of DDX3, as an oncogene or tumor suppressor, in cancer progression (Review). Oncol. Rep. *39*, 883–892.

30. Lin, T.-C. (2019). DDX3X Multifunctionally Modulates Tumor Progression and Serves as a Prognostic Indicator to Predict Cancer Outcomes. Int. J. Mol. Sci. *21*, 281.

31. Riva, V., and Maga, G. (2019). From the magic bullet to the magic target: exploiting the diverse roles of DDX3X in viral infections and tumorigenesis. Future Med. Chem. *11*, 1357–1381.

32. Zhao, L., Mao, Y., Zhao, Y., and He, Y. (2016). DDX3X promotes the biogenesis of a subset of miRNAs and the potential roles they played in cancer development. Sci. Rep. *6*, 32739.

33. Detre, S., Saclani Jotti, G., and Dowsett, M. (1995). A "quickscore" method for immunohistochemical semiquantitation: validation for oestrogen receptor in breast carcinomas. J. Clin. Pathol. *48*, 876–878.